Field-Directed Micro-Casting of Non-Spherical Nanostructures: Overcoming High-Temperature Spheroidization for Bio-Inspired Design

Yao Li, Longlong Qiao†, Yuxin Liu, Shenhao Wang, Yifei Xue, Lin Chen, Yilun Cao, Huiwu Yu*

School of physics, Northwest University, Xi'an 710127, China

*Corresponding author email: yuhuiwu@nwu.edu.cn

Heating-Melting-Evaporation (HME) model

The particle HME model was first proposed by Takami et al. and subsequently advanced by Pyatenko et al. Utilizing this model, we calculated the required laser energy for Fe_2O_3 particles of different sizes. The laser energy absorbed by a spherical particle with a diameter of d_p can be determined by Equation 1.

$$Q_{abs}(\lambda,d_p) = J\sigma_{abs}^{\lambda}(d_p) \quad (1)$$

In which, J is the laser energy density, and σ_{abs}^{λ} is the absorption cross-section, which can be calculated using Mie theory [48]. To compute the absorption efficiency of a spherical particle, two optical properties of the particle material must be known: the refractive index n and the extinction coefficient k, or equivalently, the real and imaginary parts of the complex refractive index [49,50]. For Fe_2O_3, the refractive index n is 2.4315, and the extinction coefficient k is 1.116.

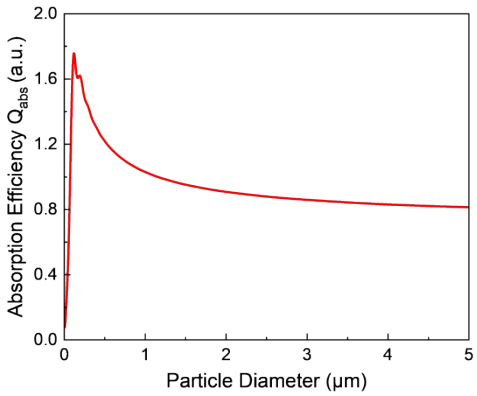

Figure S1. Absorption efficiency of spherical Fe_2O_3 particles in water, calculated for different particle sizes using Mie theory.

†These authors contributed equally to this work.

*Contact author: yuhuiwu@nwu.edu.cn

Absorption efficiency of spherical Fe_2O_3 particles of different sizes in ethanol, calculated using Mie theory. According to the HME model, the laser energy density required for the complete evaporation of a particle with a diameter of d_p can be obtained by the following equation：

$$J\sigma_{abs}^{\lambda} = m_p\left[\int_{T_0}^{T_m} c_p^s(T)dT + \Delta H_m + \int_{T_m}^{T_b} c_p^l(T)dT\right] = m_p\left[\left(H_{T_m} - H_0\right) + \Delta H_m + \left(H_{T_b} - H_{T_m}\right)\right] \quad (2)$$

As shown in Equation 2, the laser energy required to heat particles of different sizes from T_0 (298.15 K) to their melting point (T_m) and boiling point (T_b), until complete evaporation, can be determined. Here, C_p^s and C_p^l are the heat capacities of the particle in the solid and liquid states, respectively; d_p is the particle diameter; $m_p = \rho_p \frac{\pi d_p^3}{\sigma}$ is the particle mass; T_0 is the initial particle temperature; T_m is the melting temperature; T_b is the boiling temperature; ΔH_m is the enthalpy of fusion; and $H_T - H_{T_0}$ is the relative enthalpy.

Based on the above equation, the critical values of laser energy density required for different phase transitions (onset of melting, complete melting) of a material can be calculated. Figure 3(a) presents a phase diagram where these critical laser energy density values are plotted as a function of the Fe_2O_3 particle diameter. The physical and thermodynamic constants used in Equation (2) are listed in Table S1.

In the experiments, a magnetic field was introduced prior to laser irradiation, causing the nanoparticles to rotate. The nanoparticles were then irradiated with a laser energy density calculated to be within the range from the onset of melting to complete melting. This irradiation caused the particles to melt, and under the influence of the magnetic field, the molten nanoparticles deformed. Conversely, when irradiated with a laser energy density outside this specific range, the particles did not melt and, consequently, no deformation occurred.

†These authors contributed equally to this work.

*Contact author: yuhuiwu@nwu.edu.cn

Table S1. Thermodynamic data used in the calculations.

Material	ρ g/cm^3	T_m K	H_{Tm}-H_{298} KJ/mol	$\Delta H_m(T_m)$ KJ/mol
Fe_2O_3	5.24	1800	217.583	167

Cooling Model

The characteristic cooling time for droplets, estimated as R^2/κ (where R is the droplet radius and κ is the thermal diffusivity), is derived from the fundamental principles of heat conduction. This estimation method is widely applied in various thermal management and heat transfer analyses. As a universal estimation approach based on the basic principles of heat conduction, it aims to predict the temperature response and cooling behavior of objects under specific conditions by solving the heat conduction equation [51].

In the analysis of droplet cooling processes, heat conduction is one of the core mechanisms. When a droplet is deposited on a high-temperature surface, heat is transferred from the surface to the interior of the droplet through conduction, influencing its evaporation characteristics and lifetime. For droplets in a cooling environment, heat is conducted from the interior of the droplet to its surface and dissipated to the surrounding environment through convection, evaporation, and radiation. For instance, at the microscale, processes such as droplet spreading, quenching, solidification, and cooling on hot surfaces involve complex heat conduction mechanisms [52].

Based on the above relationship, a graph of droplet size versus characteristic cooling time can be plotted, as shown in Figure 2(f). The droplet size range investigated in this experiment is 100 nm to 5 μm, with corresponding characteristic cooling times calculated to be approximately 10 ns to 25 μs. This range is indicated by the solid line in the figure.

†These authors contributed equally to this work.

*Contact author: yuhuiwu@nwu.edu.cn

Numerically simulating droplet deformation.

In this study, the level-set method is employed to simulate the flow field involving a rotating droplet. We solve the constant-viscosity, incompressible Navier-Stokes equations in a rotating reference frame, which describe the fluid flow and include the force balance and mass conservation equations:

$$\rho\left(\frac{\partial u'}{\partial t'} + u' \cdot \nabla' u'\right) = -\nabla p' + \eta \nabla'^2 u + \rho\omega'^2 r' + 2\rho\omega' u' \times \hat{k} + \rho\frac{\partial \omega'}{\partial t'} r' \times \hat{k} \nabla' \cdot u' = 0 \tag{3.1}$$

$$\nabla' \cdot u' = 0 \tag{3.2}$$

In the equations, the superscript " ' " denotes dimensionless variables. The dependent variable u' is the fluid velocity, and p' is the pressure; r' is the radial vector originating from the axis of rotation, and t' is time. The axis of rotation is fixed along the z-axis, $\hat{k}$ is the unit vector in the z-direction, and η is the dynamic viscosity of the fluid. On the right-hand side of Equation (3.1), the terms represent the pressure gradient, viscous force, centrifugal force, and Coriolis force, respectively.

Figure S2 shows a schematic diagram of the simulation domain and the rotating droplet. The simulation domain is a three-dimensional rectangular region measuring 30×30×20 μm³, with an initially spherical droplet of radius 5 μm placed at its center. The droplet's interior (liquid phase) uses the physical properties of Fe_2O_3: density ρ = 5340 kg/m³, viscosity η = 0.03 Pa·s, and surface tension γ = 0.001 N/m. The droplet's exterior (gas phase) uses the physical properties of air: density ρ = 1.166 kg/m³ and viscosity η = 1.819×10^{-5} Pa·s.

†These authors contributed equally to this work.

*Contact author: yuhuiwu@nwu.edu.cn

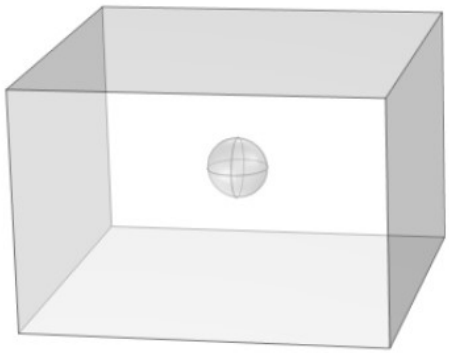

Figure S2 Simulated structure of a droplet rotating in a magnetic field.

Table S2 Force balance during the rotational deformation of a droplet in a magnetic field.

ω_x	ω_y	Numerical value	Direction of the Resultant Force	Simulation Results
+	+	$\omega_x=\omega_y$	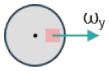	
+	+	$\omega_x\neq\omega_y$	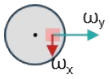	
—	+	$\lvert\omega_x\rvert=\lvert\omega_y\rvert$	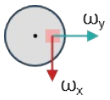	
—	—	$\omega_x=\omega_y$		

†These authors contributed equally to this work.

*Contact author: yuhuiwu@nwu.edu.cn

The Influence of Rotating Magnetic Field Frequency and Intensity on the Morphology of Molten α-Fe_2O_3 Nanoparticles

To investigate the effects of frequency and magnetic field intensity on molten α-Fe_2O_3 nanoparticles, this study conducted pulsed laser irradiation experiments on α-Fe_2O_3 nanoparticles under rotating magnetic fields with varying frequencies and intensities. The frequencies used from top to bottom in the left column are 50 Hz, 100 Hz, 150 Hz, 200 Hz, and 250 Hz, respectively; while the corresponding magnetic field intensities from top to bottom in the right column are 10 Gs, 20 Gs, 50 Gs, 70 Gs, and 150 Gs, respectively. The corresponding morphological results are presented in Figure S3.

†These authors contributed equally to this work.

*Contact author: yuhuiwu@nwu.edu.cn

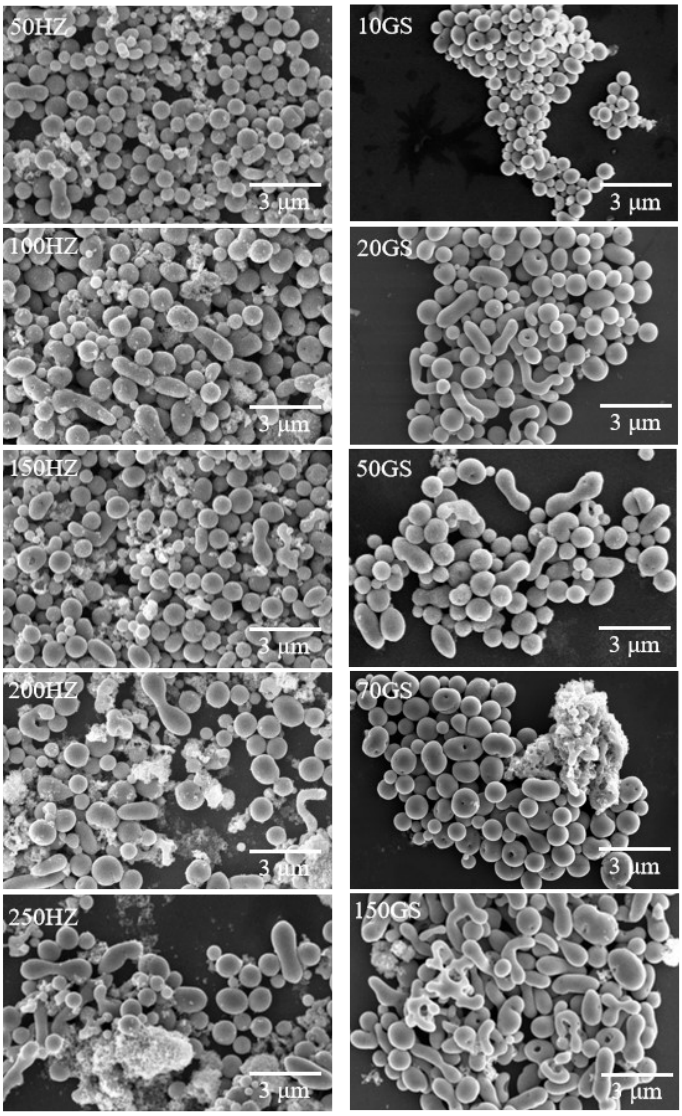

Figure S3 SEM images of α-Fe_2O_3 nanoparticles after pulsed laser irradiation, as a function of magnetic field frequency and intensity.

An increase in magnetic field intensity enhances the magnetization of the nanoparticles, promoting magnetic attraction and aggregation among them. These aggregates subsequently fuse and grow under laser irradiation, favoring the formation of larger dumbbell-shaped structures.

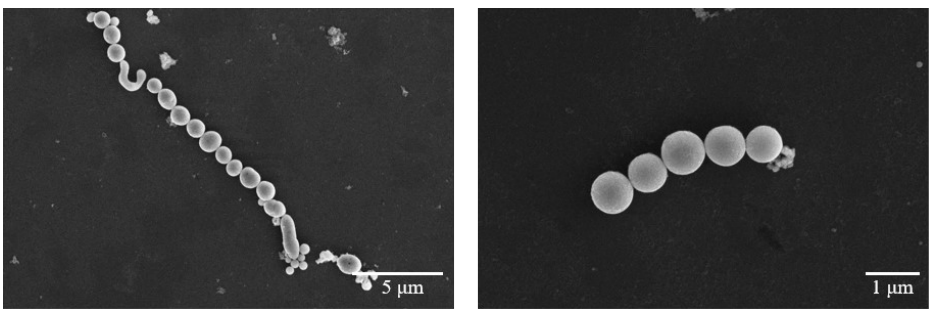

†These authors contributed equally to this work.

*Contact author: yuhuiwu@nwu.edu.cn

Figure S4 presents SEM images of the interconnected α-Fe_2O_3 nanoparticles, showing the products obtained under a magnetic field intensity of 20 Gs at frequencies of 200 Hz and 250 Hz, respectively.

XPS analysis of the products synthesized from α-Fe_2O_3 in different liquid media.

To investigate the influence of different liquid media on the deformation behavior of α-Fe_2O_3 nanoparticles, this study subjected the samples to pulsed laser irradiation using water and ethanol as the respective media. Subsequently, XPS valence state analysis was performed on the resulting products (Figure S5) to elucidate how the liquid media affect the morphological evolution mechanism of the α-Fe_2O_3 nanoparticles by modulating viscosity.

†These authors contributed equally to this work.

*Contact author: yuhuiwu@nwu.edu.cn

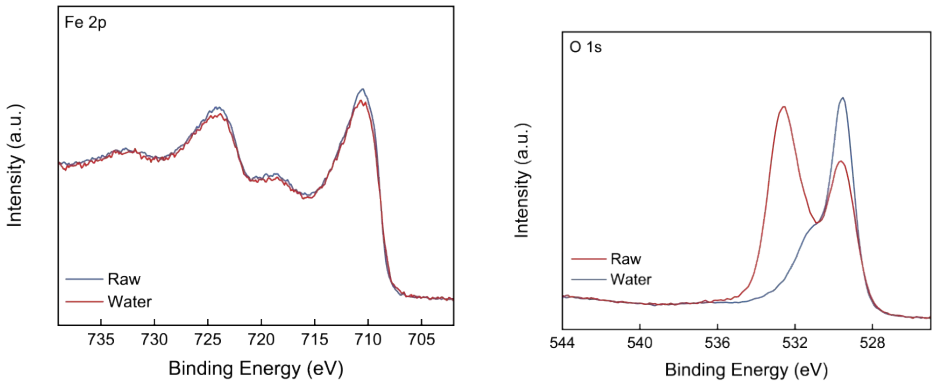

Figure S5 (a) XPS of the product from α-Fe_2O_3 in water; (b) XPS of the product from α-Fe_2O_3 in ethanol.

†These authors contributed equally to this work.

*Contact author: yuhuiwu@nwu.edu.cn